Electronic structure, phonons, and thermal properties of ScN, ZrN, and HfN: A first-principles study

Bivas Saha, Jagaran Acharya, Timothy D. Sands, and Umesh V. Waghmare

Citation: Journal of Applied Physics **107**, 033715 (2010); doi: 10.1063/1.3291117
View online: http://dx.doi.org/10.1063/1.3291117
View Table of Contents: http://scitation.aip.org/content/aip/journal/jap/107/3?ver=pdfcov
Published by the AIP Publishing

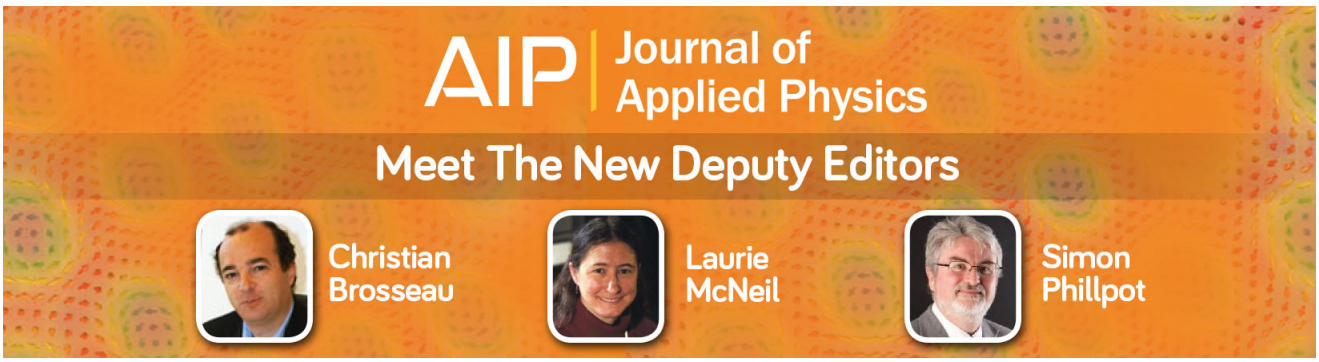

Electronic structure, phonons, and thermal properties of ScN, ZrN, and HfN: A first-principles study

Bivas Saha,[1,2] Jagaran Acharya,[3] Timothy D. Sands,[4] and Umesh V. Waghmare[2,a)]
[1]*Chemistry and Physics of Materials Unit, Jawaharlal Nehru Centre For Advanced Scientific Research, Jakkur, Bangalore 560064, India*
[2]*Theoretical Sciences Unit, Jawaharlal Nehru Centre For Advanced Scientific Research, Jakkur, Bangalore 560064, India*
[3]*Central Department of Physics, Tribhuvan University, Kathmandu, 8212 Nepal*
[4]*School of Materials Engineering, School of Electrical and Computer Engineering and Birck Nanotechnology Centre, Purdue University, West Lafayette, Indiana 47907, USA*

(Received 7 October 2009; accepted 14 December 2009; published online 8 February 2010)

With a motivation to understand microscopic aspects of ScN, ZrN, and HfN relevant to the thermoelectric properties of nitride metal/semiconductor superlattices, we determine their electronic structure, vibrational spectra and thermal properties using first-principles calculations based on density functional theory with a generalized gradient approximation of the exchange correlation energy. We find a large energy gap in the phonon dispersions of metallic ZrN and HfN, but a gapless phonon spectrum for ScN spanning the same energy range, this suggests that a reduced thermal conductivity, suitable for thermoelectric applications, should arise in superlattices made with ScN and ZrN or ScN and HfN. To obtain an electronic energy band gap of ScN comparable to experiment, we use a Hubbard correction with a parameter U (=3.5 eV). Anomalies in the acoustic branches of the phonon dispersion of ZrN and HfN, manifested as dips in the bands, can be understood through the nesting of Fermi surface determined from our calculations. To connect with transport properties, we have determined effective masses of ScN and determined their dependence on the U parameter. Using the relaxation time approximation in the Boltzmann transport theory, we estimate the temperature dependence of the lattice thermal conductivity and discuss the chemical trends among these nitrides. © *2010 American Institute of Physics*. [doi:10.1063/1.3291117]

I. INTRODUCTION

The early transition metal mononitrides are well known for their outstanding physical properties including high hardness, mechanical strength, high melting points, and electrical conductivity that varies from metallic to semiconducting. Because of these interesting features they have attracted wide attention of researchers and are extensively used in technological applications such as hard wear-resistant coatings, diffusion barriers, and optical coatings. Recently, these materials are also being investigated to understand their potential for thermoelectric applications.[1,2] As the growing demand for alternative clean energy catalyzes research in the thermoelectric field, we believe these materials (ScN, ZrN, and HfN) may have an important role to play in future thermoelectric devices, particularly at high operating temperatures where the refractory properties of the nitrides are a distinct advantage.

Electronic structures and vibrational spectra of these materials have been topics of research[5,6,9,10] for a considerable period of time. While most of these studies were aimed at understanding their physical properties, thorough analysis with a goal of assessing their potential for thermoelectric applications is much needed. The electronic structure of ScN has been intriguing as different groups have estimated different values of the band gap ranging from the zero band gap semimetallic[3,4] state to an indirect band gap semiconductor.[5,6] Recent experiments of Gall *et al.*,[7] however, suggests an indirect Γ to X gap of 0.9 ± 0.1 eV. Most recent theoretical work by Abdallah *et al.*,[8] based on the sophisticated G_0W_0 approximation, has shown the same gap to be 0.99 ± 0.15 eV. Similarly, vibrational spectra of these materials have been calculated by Isaev *et al.*[9] and Heid *et al.*[10] Interesting phonon anomalies in the acoustic branch of ZrN and HfN are well captured in their studies, and it would be nice to understand possible reasons for such phonon behavior. To develop thermoelectric superlattices based on these nitrides, it is desirable to have a detailed comparative study of their electronic and thermal properties, which are relevant to thermoelectric behavior.

Here, we use first-principles simulations to determine electronic structures, vibrational spectra, and thermal properties of ScN, ZrN, and HfN in the rock salt structure aiming to understand (a) their miscibility, and the feasibility of growing metal/semiconductor superlattices and heterostructures, (b) the detailed nature of their electronic structures, and (c) their vibrational spectra and thermal properties, for the potential applications in thermoelectric and thermionic devices. Our first-principles based DFT calculations should be useful to experimentalists in understanding properties of superlattices and multilayers of nitride materials relevant to thermoelectric applications.

a)Electronic mail: waghmare@jncasr.ac.in.

TABLE I. Calculated lattice constant a (Å) and Bulk modulus (B) of ScN, ZrN, and HfN are presented. Results of other calculations and values of experimental data are listed on the next line after results of our calculations.

System	a (Å)	B (Mbar)
ScN	4.52	2.07
	4.50,[a] 4.51,[b] 4.50,[e] 4.44[f]	2.01,[a] 1.98,[b] 1.82±0.40 [d]
ZrN	4.59	2.89
	4.57,[a] 4.583,[b] 4.537,[g] 4.61[f]	2.64,[a] 2.50,[b] 2.85[c]
HfN	4.52	2.94
	4.54,[a] 4.54,[b] 4.52[g]	2.78,[a] 2.69,[b] 3.03[c]

[a]Reference 5.
[b]Reference 9.
[c]Reference 17.
[d]Reference 18.
[e]References 19–21.
[f]Reference 22.
[g]Reference 23.

II. METHODS

We use plane wave self-consistent field (PWSCF) implementation of density functional theory (DFT), with a generalized gradient approximation (GGA)[11,12] to exchange correlation energy and ultrasoft pseudopotential[13] to represent the interaction between ionic cores and valance electrons. PWs with a cutoff energy of 30 Ry were used to represent the electronic wave functions and PWs with an energy of 180 Ry were included for the description of charge density. Integration over the Brillouin zone is carried out using the Monkhorst–Pack scheme[14] with a $10\times10\times10$ mesh of k-points, and occupation numbers are treated according to the Methfessel–Paxton[15] scheme with a broadening of 0.003 Ry. A Hubbard U correction[25] was included along with GGA in determination of the electronic structure of ScN.

Lattice-dynamical calculations (the phonon spectrum, the density of states) are performed within the framework of the self-consistent density functional perturbation theory.[16] PWs with cutoff energies of 40 and 750 Ry were used to describe wave functions and charge density, respectively. Such a high charge density cutoff is necessary to keep the errors in vibrational frequencies minimal. In order to understand the detailed features of the phonon spectra, force constants (K) are obtained on a $4\times4\times4$ q-point mesh. The dynamical matrices at arbitrary wave vectors were obtained using fourier transform based interpolations.

The specific heat C_P and thermal conductivity $\kappa_{\alpha\beta}$ (i.e along any arbitrary $\alpha\beta$ direction) are given by Eqs. (1) and (2), respectively.

$$C_P = \frac{1}{N_q}\sum_{q\lambda}\left[k_B\left(\frac{\hbar\omega_{q\lambda}}{k_BT}\right)^2\frac{e^{(\hbar\omega_{q\lambda}/k_BT)}}{(e^{\hbar\omega_{q\lambda}/k_BT}-1)^2}\right], \quad (1)$$

$$\kappa_{\alpha\beta} = \hbar\sum_{\lambda}\int\frac{d^3q}{(2\pi)^3}v_{\alpha,\lambda}(q)v_{\beta,\lambda}(q)\omega_\lambda(q)\tau_\lambda(q) \times\left[\frac{dn_B[\omega_\lambda(q)]}{dT}\right], \quad (2)$$

where λ is the polarization vector of the normal mode, $v_{\alpha,\lambda}(q)$ and $v_{\beta,\lambda}(q)$ are the velocity of phonon along any α and β directions, respectively, $\tau_\lambda(q)$ is the relaxation time, and $n_B[\omega_\lambda(q)]$ is the Boson occupation function. The relaxation time $\tau_\lambda(q)$ is assumed to be constant and kept outside the integral. Eigenfrequencies were obtained in a dense mesh of 1000 k-points over the entire Brillouin zone, which are subsequencely used in determining derivatives of phonon frequencies.

TABLE II. Calculated energies of cation mixing in eV per formula unit. $x=0.06$ and the SICs represent different symmetry inequivalent configurations.

Multiplicity	$E_{Zr_xSc_{1-x}N}$	$E_{Sc_xZr_{1-x}N}$	$E_{Hf_xSc_{1-x}N}$	$E_{Sc_xHf_{1-x}N}$
SIC 1	−0.0516	−0.0201	−0.0706	−0.0278
SIC 2	−0.0529	−0.0197	−0.0729	−0.0280
SIC 3	−0.0535	−0.0198	−0.0743	−0.0272
SIC 4	−0.0518	−0.0191	−0.0715	−0.0273
SIC 5	−0.0533	−0.0202	−0.0738	−0.0280

To get an idea about diffusion of cations across an interface in a superlattice, we determine energy of mixing for $Zr_xSc_{1-x}N$, $Sc_xZr_{1-x}N$, $Hf_xSc_{1-x}N$, and $Sc_xHf_{1-x}N$ with $x=0.6$ by considering configurations with $2\times2\times2$ cubic supercell. There are total of 496 configurations, however analysis with site occupancy disorder technique[28] yields only five symmetry inequivalent configurations. The structures are relaxed until forces on each atom are less than 0.001 Ry/bohr, and the energy of mixing is calculated using the formula

$$E_{\text{mis}} = (E_{A_mB_nN_{m+n}} - mE_{\text{AN}} - nE_{\text{BN}})/(m+n),$$

where A and B represent transition metals, and E_{AN} is the energy of a nitride AN per formula unit, $E_{A_mB_nN_{mn}}$ is the energy of alloy composed of m formula units of AN and n formula units of BN.

III. RESULTS

A. Crystal structure

The three early transition mononitrides occur in rock salt crystal structure. Our estimates of the lattice constant and bulk moduli are compared with experimental and other theoretical values (see Table I). Our calculated values of bulk moduli are overestimated by a few to ten percent with respect to earlier GGA calculations,[5,9] but they are closer to the experimental values of ZrN and HfN.[17] For ScN, though our result is overestimated with respect to the experimental value,[18] it is within the typical GGA error and consistent with other calculations.

TABLE III. Calculated band gaps of ScN, followed by other theoretical calculations and experimental observations.

Approach	$E_{\Gamma-X}$ (eV)	E_X (eV)	E_Γ (eV)
Present GGA+U	0.89	1.86	2.93
LDA+correction (Ref. 25)	0.90	2.00	4.30
Screened exchange LDA (Ref. 4)	1.58	2.41	4.80
$(G_0W_0)_{\text{average}}$ (Ref. 5)	0.99	2.02	3.62
Experimental (Ref. 22)	1.30±0.30	3.80	2.40
Experimental (Ref. 5)	0.90±0.10		2.15

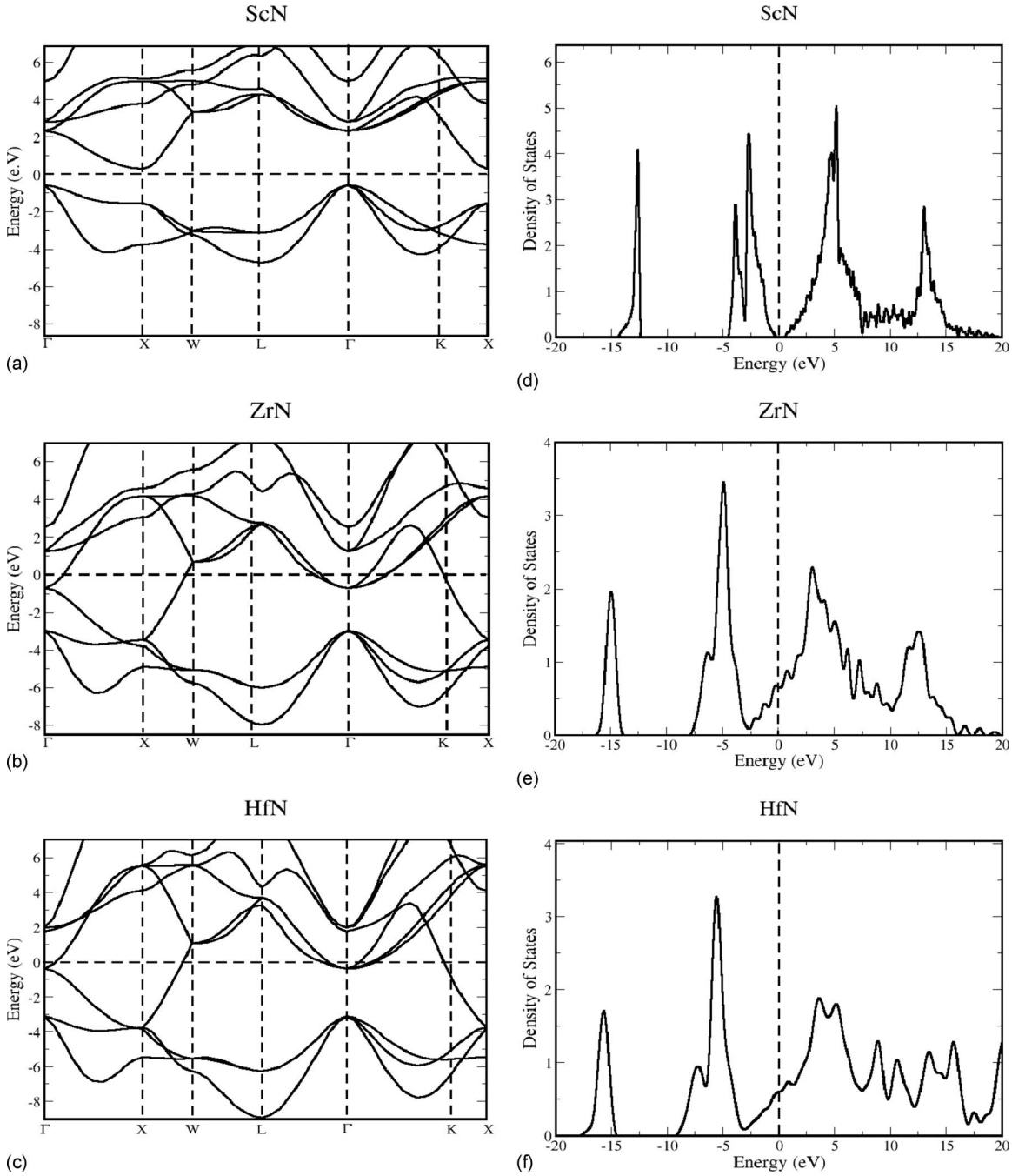

FIG. 1. Electronic structure of ScN (a), ZrN (b), and HfN (c), respectively, along high symmetry directions in the Brillouin zone. The symmetry points are Γ[000], X[010], W$\left[\frac{1}{2}10\right]$, L[111], K$\left[\frac{3}{4}\frac{3}{4}0\right]$ in the Brillouin zone, and density of electronic states of ScN (d), ZrN (e), and HfN (f). A small gap in the spectrum of ScN and small asymmetry (linear behavior) at E_F in the DOS of ZrN and HfN are evident.

Energy of mixing of all configurations are very similar (see Table II) and negative, suggesting that diffusion of transition metal atoms into nitrides at the ZrN/ScN and HfN/ScN interface is quite possible and that the superlattice interface would not be atomically sharp. Our results suggest that Zr and Hf are more likely to diffuse to ScN side than Sc diffusing to ZrN or HfN.

B. Electronic structure

As mentioned earlier, both experimental and theoretical estimates of the electronic band gap of ScN (see Table III) have been multivalued and contradicting. Freeman *et al.*[5] used screened-exchange local-density approximation (LDA) and derived an indirect Γ to X band gap of 1.58 eV, while Gall *et al.*[24] used density functional theory and the exact-exchange formalism to predict an indirect band gap of 1.6 eV. Their experimental measurement[24] shows a band gap of 1.3 ± 0.3 eV, with errors arising mainly from a large background carrier concentration causing an apparent increase in band gap. The most recent experiment of Gall *et al.*[7] suggests a band gap of 0.9 ± 0.1 eV. In this work, we have used GGA coupled with a Hubbard U parameter[25] to fit the band gaps at different locations of the dispersion spectra. Our $U = 0.0$ eV calculation shows that within GGA, ScN is semi-

TABLE IV. Calculated Band gaps (in eV) and transverse (m_t^*) and longitudinal (m_l^*) effective masses of the conduction electron at the X point (in units of m_0) with different U values for ScN. Lower part of the table shows effective masses as reported in Ref. 8. at the same point of band structure. OEPx(cLDA) is an exchange correlation functional used by them.

U (eV)	$E_{\Gamma-X}$	E_Γ	E_X	m_t^*	m_l^*
0.0	0.008	2.42	0.93	0.164	1.571
1.0	0.270	2.56	1.21	0.197	1.718
2.0	0.496	2.69	1.45	0.228	1.840
3.0	0.748	2.84	1.72	0.262	1.981
3.5	0.890	2.93	1.86	0.281	2.061
4.0	1.031	3.02	2.01	0.301	2.175
5.0	1.350	3.22	2.34	0.344	2.378
Reference 8					
OEPx(cLDA)-G_0W_0				0.189	1.483
OEPx(cLDA)				0.253	1.450
GGA				0.139	1.625

metallic in nature as found earlier by Srivastava *et al.*[26] But such a discrepancy is not surprising as DFT is known to underestimate the band gap. It can be seen that for $U=3.5$ eV, we get an indirect Γ to X gap of 0.89 eV, direct Γ point gap of 2.93 eV, and X point gap of 1.86 eV, values that are reasonably close to experimental observations and other theoretical predictions. Although the direct gap at the Γ point is underestimated with respect to other DFT based calculations, the value is only slightly higher than experimental data. The gap at the X point, on the other hand is in better agreement with previous work.

Calculated band structures of ScN (with a Hubbard U correction of $U=3.5$ eV), ZrN and HfN along high symmetry directions of the Brillouin zone [see Figs. 1(a)–1(c)] indicate that ZrN and HfN have similar band structures and both are metallic in nature with bands crossing the Fermi energy near the Γ, W and K points. Since both Zr and Hf are in the same column of the periodic table, and have the same oxidation state in their respective mononitrides with roughly the same lattice constants, such similarity in electronic structures is not surprising. Bandwidths in HfN are slightly larger than ZrN indicating larger coupling for HfN between p-states of nitrogen and d-states of the transition metals, consistent with its larger size. For ScN, semiconducting character is prominent in the band structure with a Γ to X (100 direction in Brillouin zone) band gap of 0.89 eV.

The longitudinal (m_l^*) and transverse (m_t^*) effective masses of the conduction band at the X point in the band structure of ScN are calculated by fitting a quadratic function to the corresponding band energies along $\Delta(\Gamma-X)$ and $Z(X-W)$ directions, respectively, and for different values of U [see Table IV]. Monotonic increases in effective masses with varying U parameter are observed. Typically, the d-band width decreases with increasing U parameter (bands become more flat) resulting in the increase in effective mass found here. Our estimated effective masses are overestimated with respect to Abdallah *et al.*[8] G_0W_0 calculations (see Table IV). At present we are aware of only one experimental study where a conduction band effective mass between 0.1 and 0.2 has been reported (see Ref. 27).

The density of states [see Figs. 1(d)–1(f)] shows that the metal d-band t_{2g}^3 and e_g^2 states are split up in all three cases. The effect of splitting is most pronounced in the case of ScN, the peaks of t_{2g}^3 and e_g^2 states are separated by 8 eV. These peaks in ZrN are separated by 9.5 eV, and the splitting in HfN is slightly weaker. Another notable feature of the density of states (DOS) is that the 2s-bands of nitrogen in ZrN are shifted by 2.5 eV with respect to those in ScN and this shift is 2.8 eV in HfN. This should be relevant to estimation of valence band offsets in metal/semiconductor superlattices based on these nitrides.

To determine the nature of electronic states in valence and conduction bands, we visualize the electronic wave functions of the highest occupied (valence band) and lowest unoccupied (conduction) states at Γ point (see Fig. 2). The valence bands of ScN comprise primarily of the p-states of nitrogen and the lowest conduction bands are made of xy-type (t_{2g}) orbitals of Sc, as expected in octahedral coordination. For ZrN and HfN, both valence and conduction bands (which overlap with each other) are based on mostly d-states of the transition metal (see these states of ZrN in Fig. 2). The overlap with p-states of nitrogen is reflected in the deviation in the shape of these states (see Fig. 2) from that of purely d-states.

Fermi surfaces of ZrN and HfN consist of three branches (see results for ZrN in Fig. 3, those for HfN are very similar). The branch with the largest area [see Fig. 3(a)] represents a band crossing the Fermi energy near the W and K points of the Brillouin zone (see the electronic band structure Fig. 1). The other two branches of the Fermi surface [see Figs. 3(b) and 3(c)] are smaller, and correspond to the two bands that are crossing the Fermi energy near the Γ point. We will find the features of the Fermi surface presented here useful in understanding the phonon anomalies in Sec. III C.

C. Phonons

A characteristic feature of the phonon dispersion of ScN (see Fig. 4) is the splitting of the longitudinal optical (LO) and transverse optical (TO) modes at the Γ point, which arises from long-range dipole-dipole interactions and is typical of polar semiconductors and insulators. Our estimates of the electronic dielectric constant $\epsilon(\infty)$ and Born effective charge of ScN are 12.9 and 4.35, respectively, giving an LO-TO splitting of $\Delta\omega_{\text{LO-TO}}=335$ cm^{-1}. The electronic dielectric constant, typically overestimated in DFT calculations, is quite comparable to that of other semiconductors like Si and GaAs. Our estimate of $\omega_{\text{LO}}^2/\omega_{\text{TO}}^2$ at the Γ point is about 5, which agrees well with Isaev *et al.*[9] estimation. Measured phonon dispersion curve of ScN is not available in the literature for comparison.

The branches of acoustic phonons of ScN are similar (albeit of slightly smaller slope) to those in rock salt oxides; they mix with optical phonons, but do not exhibit any anomaly. In contrast, there is an anomalous dip in the longitudinal acoustic modes of ZrN and HfN along the [100] (i.e.,

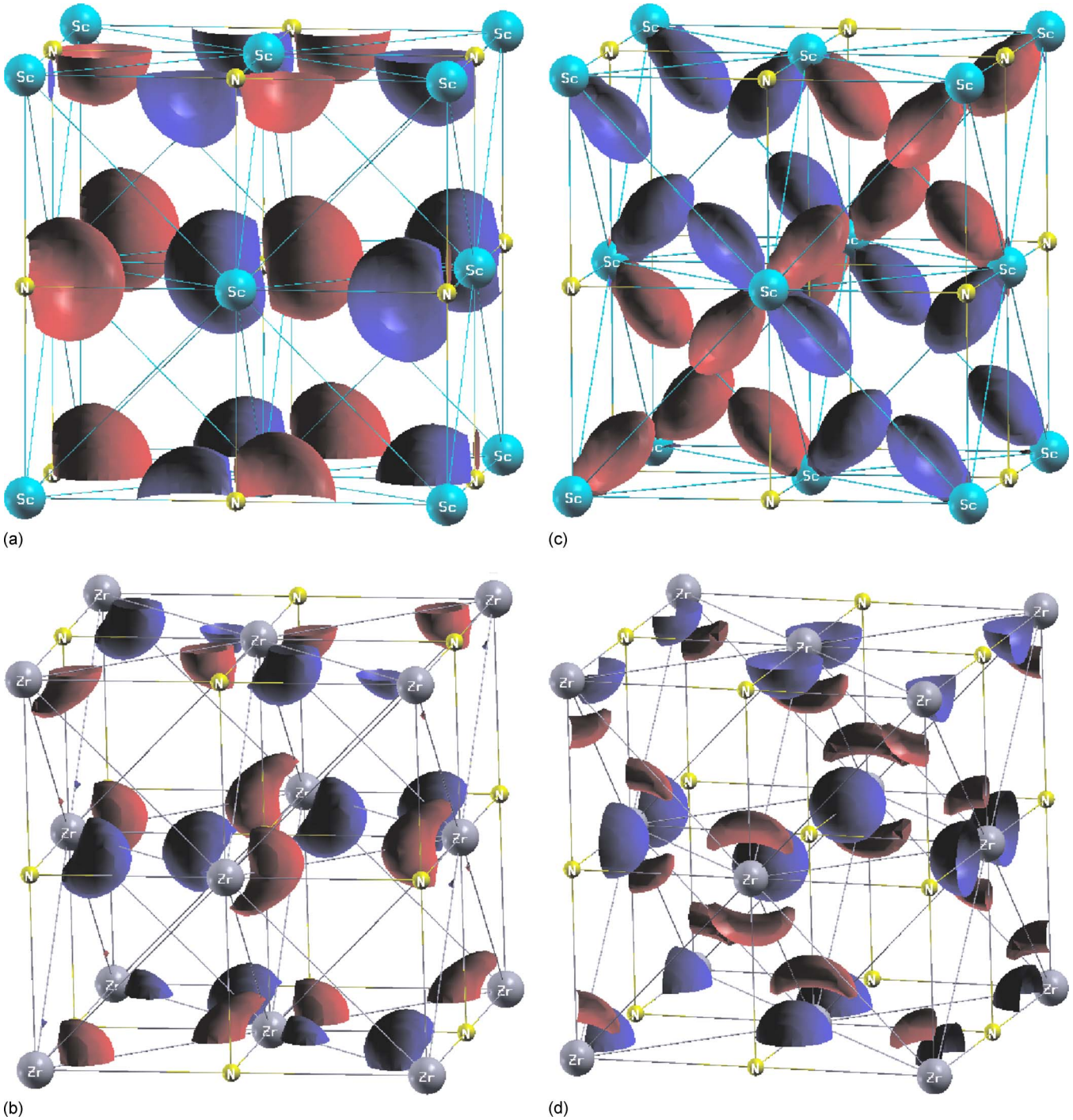

FIG. 2. (Color online) Nature of electronic states (at the Γ point) of the highest occupied valence band of ScN (a) and ZrN (b), and lowest unoccupied Conduction band (at the Γ point) for ScN (c) and ZrN (d).

Γ to X) direction (near $q=0.7$), and both the longitudinal and transverse acoustic modes along the [110] (i.e., Γ to K to X) direction. Softening of these longitudinal and transverse acoustic modes can also be observed in [111] direction (i.e., Γ to L). Phonon dispersion curves also exhibit a reverse order in LO and TO modes along [100] direction nearly at ($q=0.7$). Such anomalies in phonon frequencies can be understood with the nesting of the Fermi surface by the wave vector (q). Due to large mass difference between nitrogen and transition metal Zr and Hf atoms, there are large gaps between the acoustic branches dominated by displacements of the heavy transition metals and optical modes involving displacements of mainly nitrogen atoms. The effect is less pronounced of ScN, where such gaps in the dispersion are not observed.

While our calculated dispersion for HfN is in good agreement with experimental observations (see Ref. 26), our calculated frequencies of optical modes in ZrN differ with respect to experimental observations (see Ref. 27, in which softer frequencies are reported at the Γ point, and a much higher frequency is observed at the X point of the Brillouin zone. The observed (Ref. 27) frequency of the optical pho-

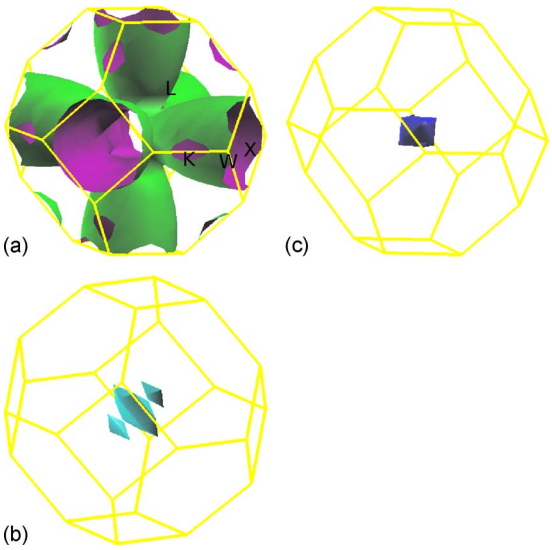

FIG. 3. (Color online) Different branches of Fermi surfaces of ZrN.

non at the Γ point of ZrN is 468 cm^{-1}, whereas our estimate of the same is 490 cm^{-1}. Other optical frequencies are approximately 5%–8% softer than experimental estimates. However, our calculated phonon dispersion compares quite well with calculations of Isaev *et al.*[9] and Heid *et al.*[10]

D. Thermal properties

Since the applications of these nitrides are expanding to thermoelectrics, we present a comparative theoretical analysis of thermal properties like specific heat and lattice thermal conductivity aiming to understand (a) the temperature dependence of the specific heat and lattice thermal conductivity and (b) the contribution of various phonon modes to thermal properties that will be useful in developing statistical thermodynamical model to predict thermal properties of their superlattices.

Our results for specific heats as a function of temperature (see Fig. 5) show that (below 300 K) HfN has the largest C_p followed by ZrN and ScN at low temperatures. This can be understood from the phonon dispersions presented earlier, acoustic branches (velocity of sound) of HfN are softer than those in ZrN and ScN. This is not surprising as these are dominated by Hf displacements and Hf has a larger mass compared to Zr and Sc. Since the specific heat at low temperature is dominated by acoustic phonons and is inversely proportional to the cube of the velocity of sound, the specific heat of HfN is the largest at low temperatures. At high temperatures, the C_p values of all the three materials, are identical to the Dulong Petit value (for diatomic system). A crossover to this classical limit is set by the effective Debye temperature. An estimate of Debye temperature (T_D) (obtained using the slope of acoustic branches in our phonon dispersion; and an effective wave vector cutoff) are about 711, 512, and 326 K for ScN, ZrN, and HfN, respectively. We note that the specific heat of HfN remains higher than that of ScN and ZrN at all temperatures.

We now analyze the lattice thermal conductivity using Boltzmann transport theory. Since we have not determined anharmonic interactions between phonons, it is not possible

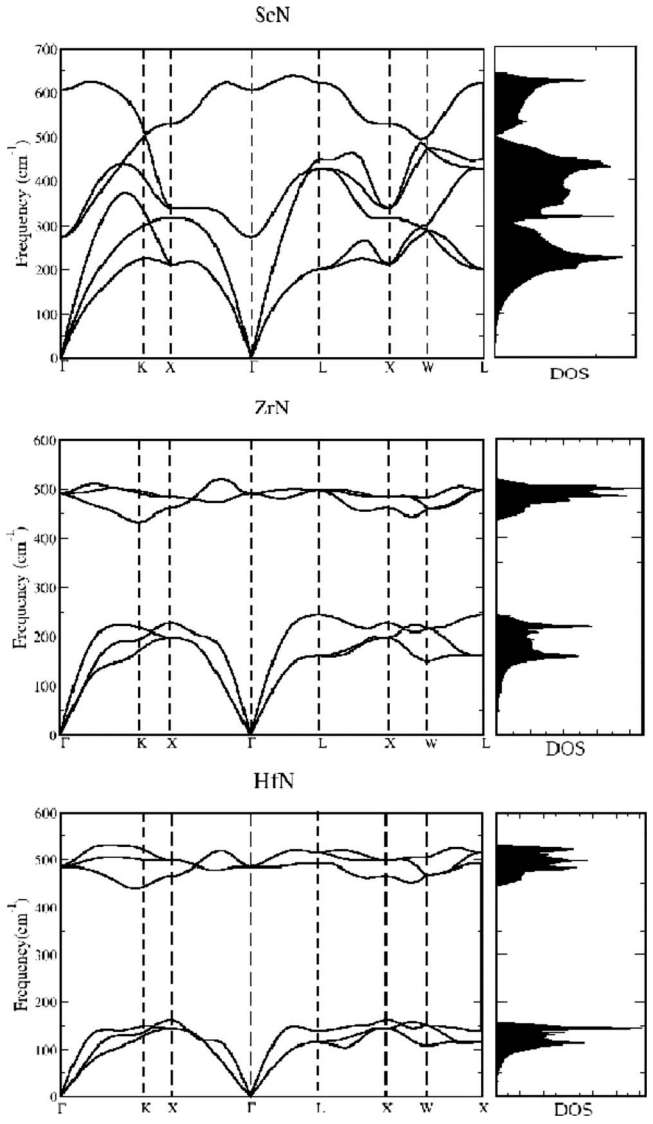

FIG. 4. Calculated phonon dispersion curve and density of states of ScN, ZrN, and HfN in rock salt structure. First columns has the phonon dispersion curves, while the right column has phonon DOS with same frequency scale. Gaps in the phonon spectra of ZrN and HfN are evident.

to estimate scattering time. We assume that the scattering time is constant for all phonons and compare the thermal conductivities of the three nitrides, including only the effects of DOS and group velocity of phonons. Our results for temperature dependent lattice thermal conductivity (see Figs. 6 and 7) show that κ of ScN is larger than the other two nitrides above 30 K. Since ScN is semiconducting in nature, the estimated C_p and κ should be roughly equal to the total values as the electronic contribution will be very small. It is clear from the phonon density of states (see Fig. 4) that a large number of phonons (both acoustic and optical phonons) of ScN fall in the mid-frequency range [250–500 cm^{-1}]. As a result, its lattice thermal conductivity is much higher than that of ZrN and HfN, where a large gap in the energies of acoustic and optical phonons is observed. While the gap between acoustic and optical modes is 191 cm^{-1} for ZrN, it is 283 cm^{-1} for HfN, and a cross over among thermal conduc-

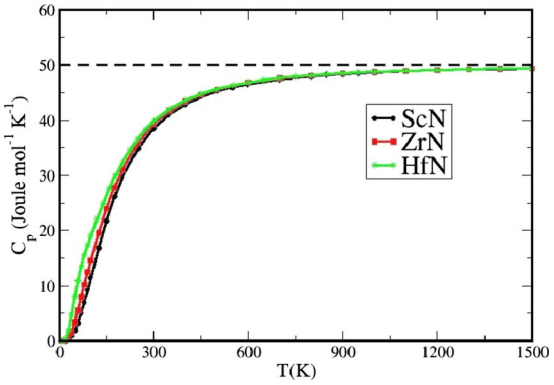

FIG. 5. (Color online) Lattice specific heat as a function of temperature of the three nitrides. Horizontal line represents classical Dulong–Petit limit of C_p.

tivities is observed at about 30 K below, which HfN has the largest thermal conductivity dominated by its acoustic phonons.

IV. POTENTIAL FOR THERMOELECTRIC APPLICATIONS

Having discussed the physical properties of these nitrides in previous sections, we now comment on their potential use in making superlattices for thermoelectric applications. First of all, closely matched lattice constants (nearly perfect matching in the case of ScN and HfN, and ≈1.5% lattice mismatch between ScN and ZrN) augur well for growing multilayers and superlattices, although one should be careful in analyzing their interfaces as the negative energy of miscibility suggests a tendency for diffusion of cations across the interface, potentially leading to diffuse interfaces at the atomic scale. Second, from our results for their electronic properties, these materials seem ideal for growing metal/semiconductor [ZrN/ScN and HfN/ScN] superlattices, with a moderate band gap of ScN that can be utilized for controlling the Schottkey barrier height, a key parameter for the energy filtering mechanism that can be used to tune the Seebeck coefficient and optimize the power factor.[1,29] Third, the proposed nitride metal/semiconductor superlattices should also act as phonon filters for reduction of lattice thermal conductivity, due to large gap in the phonon spectra of ZrN and HfN, mismatching with a high density of phonons

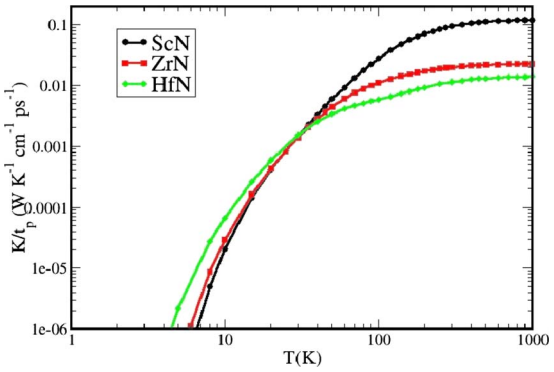

FIG. 6. (Color online) Estimated lattice thermal conductivity as a function of temperature of ScN, ZrN, and HfN.

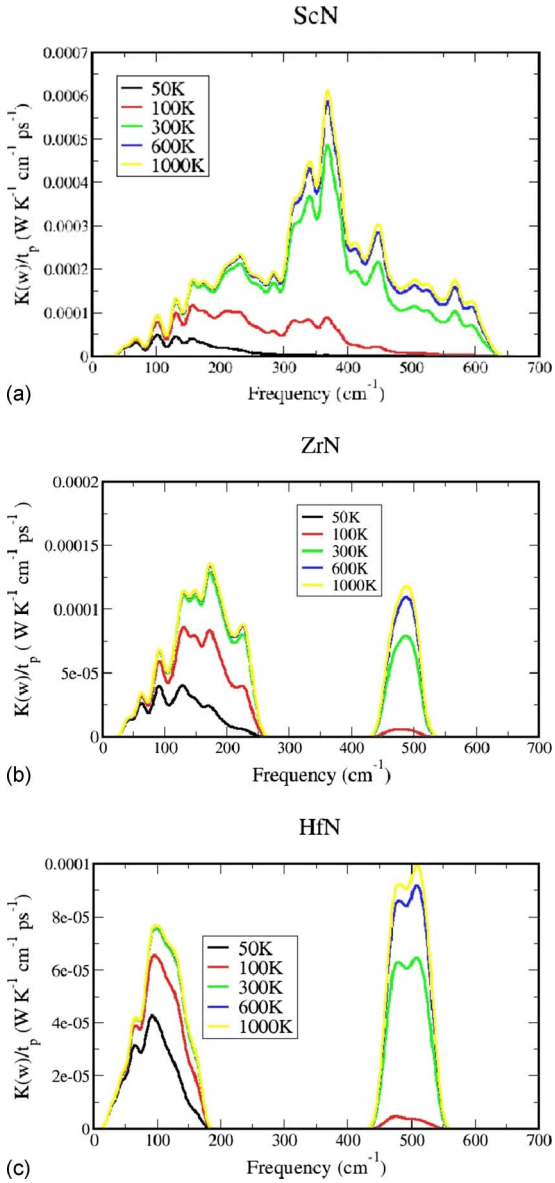

FIG. 7. (Color online) Phonon contribution to thermal conductivity of ScN (a), ZrN (b), and HfN (c), at various temperatures, as a function of phonon frequencies.

of ScN in the same range of energy. We predict that HfN/ScN superlattices should have smaller lattice thermal conductivity compared to ScN/ZrN as the extent of the gap between acoustic and optical phonons is larger for HfN than ZrN. Surely, more work on superlattices of these nitrides is desirable to assess their effectiveness for thermoelectric applications. Our results here should form a starting point for development of models and further analysis of superlattices.

V. CONCLUSION

In conclusion, we have presented a comparative first-principles theoretical analysis of electronic structure, vibrational spectra and thermal properties of bulk ScN, ZrN, and HfN, with a motivation to assess their potential for thermoelectric applications. While ScN is a semiconductor with a small electronic band gap, ZrN and HfN are metals exhibiting a large gap in their phonon spectra. Thus, metal/

semiconductor superlattices based on these nitrides can act as filters for both electrical charge and phonon thermal transport, with implications for enhancement in their thermoelectric properties. While typical DFT calculations fail to capture the semiconducting electronic gap of ScN, we demonstrate that inclusion of a relatively cost-effective Hubbard U-correction with an appropriate choice of $U=3.5$ eV can be used to obtain a reasonable description of the electronic structure of ScN. Anomalies in the phonon dispersion of metallic ZrN and HfN, manifested as dips in acoustic branches, can be understood through the nesting of the Fermi surface as determined from our calculations. To connect with transport properties, we have determined electronic effective masses of the conduction band in ScN and used Boltzmann transport theory to estimate the temperature dependence of the lattice thermal conductivity. Analysis of the temperature dependence and chemical trends in thermal transport properties of these nitrides should be useful in further work on nanoscale superlattices of these nitrides with enhanced thermoelectric properties.

ACKNOWLEDGMENTS

We thank IUS-STF for supporting collaborative interaction between JNCSAR and Purdue. Bivas Saha thanks JNCASR for a fellowship, J Acharya thanks a TWAS fellowship to support his visit to JNCASR and UVW thanks funding from a DAE Outstanding Researcher Grant.

[1]M. Zebarjadi, Z. Bian, R. Singh, A. Shakourie, R. Wortman, V. Rawat, and T. Sands, J. Electron. Mater. **38**, 960 (2009).
[2]V. Rawat, Y. Koh, D. Cahill, and T. Sands, J. Appl. Phys. **105**, 024909 (2009).
[3]G. Travaglini, F. Marabelli, R. Monnier, E. Kaldis, and P. Wachter, Phys. Rev. B **34**, 3876 (1986).
[4]R. Monnier, J. Rhyner, T. M. Rice, and D. D. Koelling, Phys. Rev. B **31**, 5554 (1985).
[5]C. Stampfl, W. Mannstadt, R. Asahi, and A. J. Freeman, Phys. Rev. B **63**, 155106 (2001).
[6]W. R. L. Lambrecht, Phys. Rev. B **62**, 13538 (2000).
[7]H. A. Al-Brithen, A. Smith, and D. Gall, Phys. Rev. B **70**, 045303 (2004).
[8]A. Qteish, P. Rinke, M. Scheffler, and J. Neugebauer, Phys. Rev. B **74**, 245208 (2006).
[9]E. I. Isaev,S. I. Simak, I. A. Abrikosov, R. Ahuja, Y. K. Vekilov, M. I. Katsnelson, A. I. Lichtenstein, and B. Johansson, J. Appl. Phys. **101**, 123519 (2007).
[10]R. Heid, K.-P. Bohnen, B. Renker, T. Wolf, and H. Schober, Phys. Rev. B **71**, 092302 (2005).
[11]J. P. Perdew, K. Burke, and M. Ernzerhof, Phys. Rev. Lett. **77**, 3865 (1996).
[12]X. Hua, X. Chen, and W. A. Goddard III, Phys. Rev. B **55**, 16103 (1997).
[13]D. Vanderbilt, Phys. Rev. B **41**, 7892 (1990).
[14]H. J. Monkhorst and J. D. Pack, Phys. Rev. B **13**, 5188 (1976).
[15]M. Methfessel and A. Paxton, Phys. Rev. B **40**, 3616 (1989).
[16]S. Baroni S. de Gironcoli, A. D. Corso, P. Giannozzi, Rev. Mod. Phys. **73**, 515 (2001).
[17]X.-J. Chen, V. V. Struzhkin, Z. Wu, M. Somayazulu, J. Qian, S. Kung, A. N. Christensen, Y. Zhao, R. E. Cohen, H.-K. Mao, and R. J. Hemley, Proc. Natl. Acad. Sci. U.S.A. **102**, 3198 (2005).
[18]D. Gall, I. Petrov, N. Hellgren, L. Haltman, J. E. Sundgren, and J. E. Green, J. Appl. Phys. **84**, 6034 (1998).
[19]W. Lengauer, J. Solid State Chem. **76**, 412 (1988).
[20]V. A. Gubanov, Z. W. Lu, B. M. Llein, and C. Y. Fong, Phys. Rev. B **53**, 4377 (1996).
[21]K. T. Park, K. Terakura, and N. Hamada, J. Phys. C **20**, 1241 (1987).
[22]R. W. G. Wyckoff, *Crystal Structure*, 2nd ed. (Wiley, New York, 1963), Vol. 1, p. 86.
[23]*Structure Reports*, edited by W. B. Pearson (International Union of Crystallography, Utrecht, 1993).
[24]D. Gall, M. Stadele, K. Jarrendahl, I. Petrov, P. Desjardins, R. T. Haasch, T.-Y. Lee, and J. E. Greene, Phys. Rev. B **63**, 125119 (2001).
[25]V. I. Anisimov and O. Gunnarson, Phys. Rev. B **43**, 7570 (1991).
[26]S. Duman, S. Bagci, H. M. Tutuncu, G. Ugur, and G. P. Srivastava, Diamond Relat. Mater. **15**, 1175 (2006).
[27]G. Harbeke, E. Meier, and J. P. Dismukes, Opt. Commun. **4**, 335 (1972).
[28]R. Grau-Crespo, S. Hamad, C. R. A. Catlow, and N. H. de Leeuw, J. Phys.: Condens. Matter **19**, 256201 (2007).
[29]D. Vashaee and A. Shakouri, Phys. Rev. Lett. **92**, 106103 (2004).